

The Bright Ultra-hard *XMM-Newton* Survey: WISE-MIR selection of luminous AGN

S. Mateos^{1,2}, A. Alonso-Herrero¹, F. J. Carrera¹, A. Blain², M. G. Watson²,
X. Barcons¹, V. Braito³, P. Severgnini⁴, J. L. Donley⁵, and D. Stern⁶

¹ Instituto de Física de Cantabria (CSIC-Universidad de Cantabria), Santander, Spain

² Physics and Astronomy, University of Leicester, University Road, Leicester LE1 7RH, UK

³ Istituto Nazionale di Astrofisica - Osservatorio Astronomico di Brera, Via Bianchi 46
I-23807 Merate (LC), Italy

⁴ INAF-Osservatorio Astronomico di Brera, via Brera 28, 20121 Milano, Italy

⁵ Los Alamos National Laboratory, Los Alamos, NM 87545, USA

⁶ Jet Propulsion Laboratory, California Institute of Technology, Pasadena, CA 91109, USA

Abstract

We present a highly complete and reliable mid-infrared (MIR) colour selection of luminous AGN candidates using the 3.4, 4.6, and 12 μm bands of the WISE survey. The MIR colour wedge was defined using the wide-angle Bright Ultra-Hard *XMM-Newton* Survey (BUXS), one of the largest complete flux-limited samples of bright ($f_{4.5-10\text{ keV}} > 6 \times 10^{-14} \text{ erg s}^{-1} \text{ cm}^{-2}$) “ultra-hard” (4.5–10 keV) X-ray selected AGN to date. BUXS includes 258 objects detected over a total sky area of 44.43 deg² of which 251 are spectroscopically identified and classified, with 145 being type-1 AGN and 106 type-2 AGN. Our technique is designed to select objects with red MIR power-law spectral energy distributions (SED) in the three shortest bands of WISE and properly accounts for the errors in the photometry and deviations of the MIR SEDs from a pure power-law. At $L_{2-10\text{keV}} > 10^{44} \text{ erg s}^{-1}$, where the AGN is expected to dominate the MIR emission, 97.1^{+2.2%}_{-4.8%} and 76.5^{+13.3%}_{-18.4%} of the BUXS type-1 and type-2 AGN meet the selection. Our technique shows one of the highest reliability and efficiency of detection of the X-ray selected luminous AGN population with WISE amongst those in the literature. In the area covered by BUXS our selection identifies 2755 AGN candidates detected with SNR ≥ 5 in the three shorter wavelength bands of WISE with 38.5% having a detection at 2–10 keV X-ray energies.

1 Introduction

There is strong observational evidence that active galactic nuclei (AGN) play an important role in the formation and growth of galaxies [8]. Most supermassive black hole growth takes place during an obscured quasar phase thus, to understand the evolution of galaxies and to trace the energy output due to accretion it is critical to map the history of obscured accretion.

X-ray surveys with *XMM-Newton* and *Chandra* at energies < 10 keV are sensitive to all but the most heavily obscured AGN. The ongoing Swift and INTEGRAL surveys at energies > 15 keV are providing the least biased samples of absorbed AGN. However, even these surveys are biased against the most absorbed Compton-thick AGN [3]. Surveys at mid-infrared (hereafter MIR) wavelengths ($> 5 \mu\text{m}$) are much less affected by extinction since the obscuring dust re-emits the nuclear optical-to-X-ray radiation at infrared wavelengths. Thus, MIR-based surveys can potentially trace the elusive obscured accretion missed by hard X-ray surveys [12]. MIR-based AGN selection techniques have been developed with data from the Spitzer Space Telescope Infrared Array Camera using colours and power-law selection [1, 4]. These techniques are very effective and reliable. The Wide-field Infrared Survey Explorer (WISE) has now completed the first sensitive coverage of the entire sky in the MIR [15]. Several colour-based regions, aimed at identifying luminous AGN, have already been proposed showing that WISE can robustly separate luminous AGN from normal galaxies and stars (e.g. [2, 7, 13, 10]). The all-sky WISE survey will complement the deep Spitzer surveys, aimed to characterize the accretion phenomenon in the distant Universe.

2 The Bright Ultra-hard *XMM-Newton* Survey

BUXS is one of the largest, amongst the existing *XMM-Newton* and *Chandra* surveys, complete flux-limited samples of bright ($f_{4.5-10\text{keV}} > 6 \times 10^{-14} \text{erg s}^{-1} \text{cm}^{-2}$) “ultra-hard” (4.5-10 keV) X-ray selected sources to date. BUXS is based on a subset of 381 high Galactic latitude ($|b| > 20 \text{deg}$) observations from the second *XMM-Newton* serendipitous source catalogue 2XMM [14] covering a total sky area of 44.43 deg^2 . BUXS contains 258 extragalactic sources. The current spectroscopic identification completeness is 97.3%. Of the 258 BUXS sources, 145 objects (56.2%) are identified as type-1 AGN (UV/optical emission line velocity widths $\geq 1500 \text{ km s}^{-1}$) and 106 (41.1%) as type-2 AGN (UV/optical emission line velocity widths $< 1500 \text{ km s}^{-1}$ or no emission lines). Seven sources (2.7%) remain unidentified. BUXS covers the region of the AGN redshift-luminosity parameter space that WISE will sample thus, offering a unique dataset to define a highly complete and reliable WISE based AGN selection.

3 WISE selection of AGN candidates in the BUXS fields

In the BUXS survey area there are 25206 sources detected with $\text{SNR} \geq 5$ at 3.4, 4.6, and $12 \mu\text{m}$ of which 1659 have X-ray detections. Out of the latter, 114 are associated with BUXS type-1 AGN and 81 with BUXS type-2 AGN. Figure 1 shows the MIR $\log(f_{4.6}/f_{3.4})$ versus $\log(f_{12}/f_{4.6})$ diagram for WISE objects with and without an X-ray counterpart as

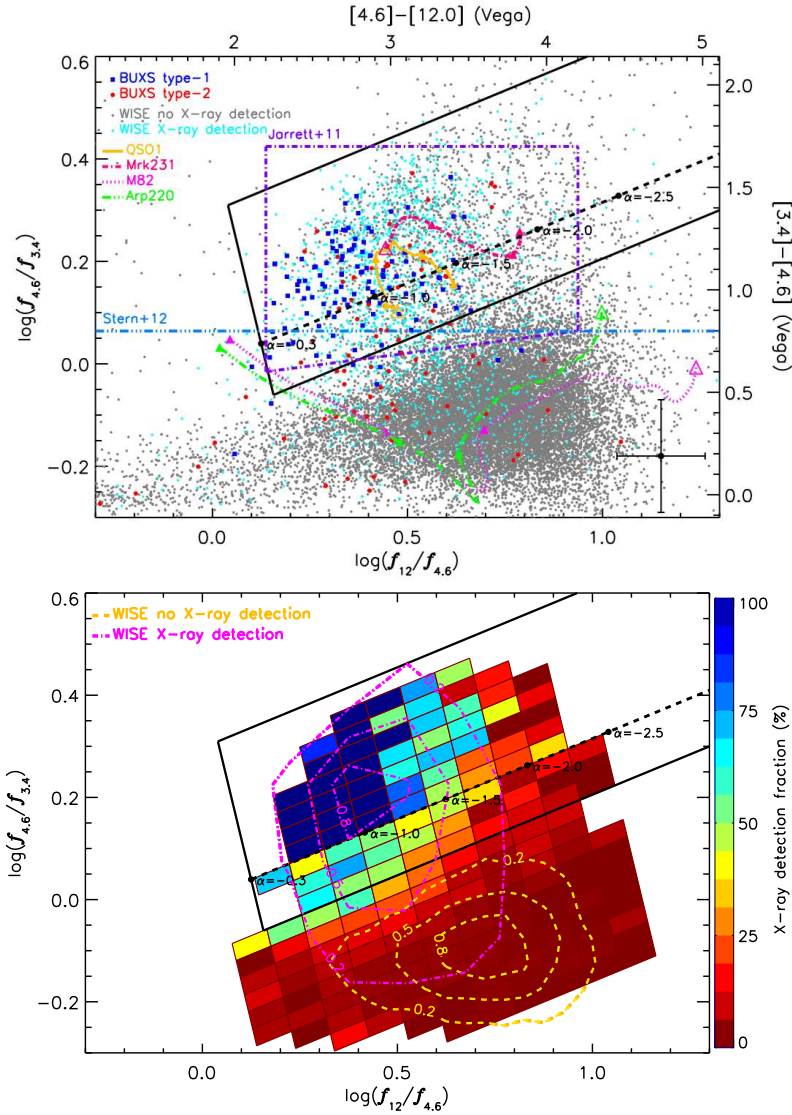


Figure 1: *Top*: MIR colours for sources detected with $\text{SNR} \geq 5$ at 3.4, 4.6, and 12 μm . Large symbols represent spectroscopically identified BUXS AGN. Small cyan and grey symbols are WISE sources in the BUXS area with and without an X-ray detection at 2–10 keV, respectively. The $0 < z \leq 1.5$ ($\Delta z = 0.5$) star-forming tracks represent M82 and the ULIRG Arp 220. The $0 < z \leq 3$ ($\Delta z = 0.5$) AGN tracks represent Mrk 231 [11] and a QSO1 template from [5] and [6]. Open symbols indicate $z = 0$. Our AGN selection wedge and power-law locus are the thick solid and dashed black lines, respectively. For comparison we show the AGN criteria defined by [7] and [13], respectively (dotted-dashed purple and light blue lines). The error bars show the typical uncertainties in MIR colours at the $\text{SNR} = 5$ limit. *Bottom*: X-ray detection fraction of WISE objects across the colour-colour plane for bins containing at least 10 sources. Dotted-dashed (magenta) and dashed (yellow) contours indicate the density of WISE sources (normalized to the peak value) with and without X-ray detection, respectively.

small cyan and grey symbols, respectively. We also marked with large blue and red symbols spectroscopically classified type-1 and type-2 AGN in the BUXS survey. The dashed line illustrates the MIR power-law locus and the values for different spectral indices. Most BUXS objects, especially type-1 AGN, are clustered near the power-law locus, in a region in the MIR colour-colour plane well separated from the stellar locus (colours near zero magnitude) and the horizontal sequence of normal galaxies (lower right part of the diagram). AGN have, on average, redder $\log(f_{4.6}/f_{3.4})$ colours than a pure power-law. This suggests some curvature in their observed 3.4 μm to 12 μm SEDs.

Figure 1 (bottom) shows the fraction of WISE sources detected in X-rays across the colour-colour diagram and the distribution of objects with and without detection in X-rays (contours). There is a clear separation between these distributions. The bulk of the MIR population not detected in X-rays overlaps with the horizontal sequence of normal galaxies, while the great majority of X-ray detected objects cluster near the power-law locus.

Our MIR-based AGN selection technique is designed to identify objects with red MIR power-law SEDs. The AGN wedge is defined to include all objects with MIR colours expected for power-law SEDs with spectral index $\alpha \leq -0.3$, properly accounting for the typical errors in the photometry at the faintest MIR fluxes (error bars in Fig. 1, top). We then increase the size of the wedge towards red $\log(f_{4.6}/f_{3.4})$ colours (upper boundary) to include all BUXS AGN and the X-ray detected WISE objects throughout the BUXS survey area with such colours. In this way we account for deviations of the 3.4 μm to 12 μm SEDs from a pure power-law. Our three-band AGN wedge is shown with the thick solid box in Fig. 1. The MIR power-law locus is defined by

$$y = 0.315 x, \quad (1)$$

where $x \equiv \log_{10} \left(\frac{f_{12\mu\text{m}}}{f_{4.6\mu\text{m}}} \right)$ and $y \equiv \log_{10} \left(\frac{f_{4.6\mu\text{m}}}{f_{3.4\mu\text{m}}} \right)$. The top and bottom boundaries of the wedge are obtained by adding y -axis intercepts of +0.297 and -0.110 , respectively. The MIR power-law $\alpha = -0.3$ bottom-left limit corresponds to

$$y = -3.172 x + 0.436. \quad (2)$$

Our three-band AGN wedge identifies 2755 AGN candidates in the BUXS area, of which 1062 (38.5%) are detected in X-rays. Out of the latter, 105 are associated with BUXS type-1 AGN and 38 with BUXS type-2 AGN.

The X-ray detection fraction in the wedge increases with the depth of the X-ray observations as long X-ray exposures are required to detect intrinsically less luminous and/or heavily obscured AGN [9]. Still, a substantial fraction of our MIR AGN candidates are undetected at 2–10 keV energies with the typical exposures in the 2XMM catalogue. These objects that have the reddest overall MIR colours in the AGN wedge, are the best candidates to account for the most heavily absorbed luminous AGN missed by hard X-ray surveys.

3.1 AGN selection completeness

Figure 2 shows the fraction of BUXS AGN that meet our MIR colour cuts as a function of their intrinsic 2–10 keV luminosity. The completeness of our selection is a strong function of

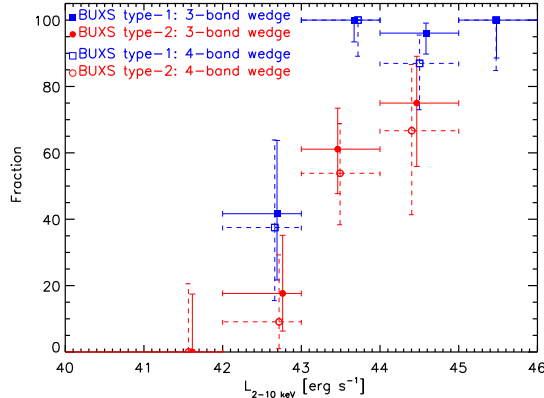


Figure 2: Fraction of BUXS AGN that meet our MIR selection as a function of their intrinsic 2–10 keV luminosity. For comparison we show the results of a selection using the three shorter wavelength bands of WISE (filled symbols) and the complete four bands (open symbols).

luminosity. This result reflects the fact that objects with MIR colours not dominated by the thermal emission from the AGN will be missed by our selection. This effect is more important for low-luminosity AGN, especially if these sources are affected by large dust extinction at the shortest wavelengths of WISE. In these objects the starlight from the host galaxy will dominate their MIR emission. At $L_{2-10 \text{ keV}} < 10^{44} \text{ erg s}^{-1}$, $84.4^{+7.4}_{-10.0}\%$ and $39.1^{+10.1}_{-9.5}\%$ of the type-1 and type-2 AGN, respectively meet the selection. At $L_{2-10 \text{ keV}} \geq 10^{44} \text{ erg s}^{-1}$ the MIR selection efficiency increases to $97.1^{+2.2}_{-4.8}\%$ and $76.5^{+13.3}_{-18.4}\%$ for type-1 and type-2 AGN, respectively. The significantly smaller value of the selection completeness obtained for type-2 AGN at $L_{2-10 \text{ keV}} < 10^{44} \text{ erg s}^{-1}$ compared to that for type-1 AGN is mainly due to the different luminosity distributions of the two classes of AGN. The type-2 AGN population in BUXS is dominated by objects with $L_{2-10 \text{ keV}} < 10^{44} \text{ erg s}^{-1}$ ($\sim 79\%$ versus $\sim 39\%$ for type-1 AGN). At such luminosities many AGN have relatively blue colours at the shortest WISE wavelengths (i.e. host-dominated) and thus lie outside the MIR AGN wedge.

3.2 Comparison with other WISE selection techniques

Within the BUXS survey area our three-band MIR colour selection identifies 2755 AGN candidates, of which 38.5% are detected in X-rays. For comparison, the X-ray detection fraction of WISE objects that meet the [7] colour-based AGN selection (indicated in Fig. 1) is 33.4%. At red MIR colours their selection enters the sequence of low redshift normal galaxies increasing the expected number of contaminants. [13] proposed an AGN selection using a [3.4]–[4.6] colour cut ($\log(f_{4.6}/f_{3.4}) > 0.06$) and a $4.6 \mu\text{m}$ flux threshold of $160 \mu\text{Jy}$. Their argument was that the inclusion of the longer wavelength WISE data would increase the reliability of the AGN selection but at the cost of reducing the completeness. Figure 1

shows that such [3.4]–[4.6] colour cut also enters the locus of low redshift normal galaxies at red $\log(f_{12}/f_{4.6})$ colours reducing the reliability of their selection as suggested by the lower X-ray detection fraction of WISE sources in the BUXS area that meet their criteria (31.8%). The *XMM-Newton* pointings used to build BUXS span a broad range of ecliptic latitudes and thus the depth of the WISE survey varies across the BUXS fields. The [13] AGN selection was defined using the COSMOS field located at low ecliptic latitude and thus, the MIR data are close to the minimum depth of the WISE survey. At such shallow depths and using the [13] 160 μJy flux threshold at 4.6 μm , many of the star-forming contaminants will be too faint to be detected, thereby increasing the reliability of the [13] selection. Although BUXS likely samples fainter objects than those best targeted at the shallow depth of WISE, we find that $\sim 98\%$ of the AGN have MIR detections with $\text{SNR} \geq 5$ at 3.4 μm and 4.6 μm . This fraction only decreases to $\sim 77\%$ if we require 12 μm detections with $\text{SNR} \geq 5$. In conclusion, over the range of MIR depths of the WISE survey in the BUXS fields, our proposed selection suffers less contamination from star-forming galaxies than provided by a simple [3.4]–[4.6] color cut, while only marginally reducing completeness.

It is clear that our MIR colour selection is a good compromise between completeness and the crucial high reliability required to obtain a clean sample of powerful AGN at the different depths of the WISE survey. Furthermore, going down to detections with $\text{SNR} \geq 5$, we reach a much higher efficiency of detection of the AGN population in the reddest MIR colours, many of which could be heavily obscured/extincted AGN.

References

- [1] Alonso-Herrero, A., Pérez-González, P. G., Alexander, D. M., et al. 2006, *ApJ*, 640, 167
- [2] Assef, R. J., Kochanek, C. S., Brodwin, M., et al. 2010, *ApJ*, 713, 970
- [3] Burlon, D., Ajello, M., Greiner, J., et al. 2011, *ApJ*, 728, 58
- [4] Donley, J. L., Koekemoer, A. M., Brusa, M., et al. 2012, *ApJ*, 748, 142
- [5] Glikman, E., Helfand, D. J., & White, R. L. 2006, *ApJ*, 640, 579
- [6] Hernán-Caballero, A. & Hatziminaoglou, E. 2011, *MNRAS*, 414, 500
- [7] Jarrett, T. H., Cohen, M., Masci, F., et al. 2011, *ApJ*, 735, 112
- [8] Magorrian, J., Tremaine, S., Richstone, D., et al. 1998, *AJ*, 115, 2285
- [9] Mateos, S., Barcons, X., Carrera, F. J., et al. 2005, *A&A*, 444, 79
- [10] Mateos, S., Alonso-Herrero, A., Carrera, F. J., et al. 2012, *MNRAS*, 426, 3271
- [11] Polletta, M., Weedman, D., Hönig, S., et al. 2008, *ApJ*, 675, 960
- [12] Severgnini, P., Caccianiga, A., & Della Ceca, R. 2012, *A&A*, 542, 46
- [13] Stern, D., Assef, R. J., Benford, D. J., et al. 2012, *ApJ*, 753, 30
- [14] Watson, M. G., Schröder, A. C., Fyfe, D., et al. 2009, *A&A*, 493, 339
- [15] Wright, E. L., Eisenhardt, P. R. M., Mainzer, A. K., et al. 2010, *AJ*, 140, 1868